https://doi.org/10.1016/j.msea.2015.10.125

How hot is a shear band in a metallic glass?

J.G. Wang[a,b], Y. Pan[c], S.X. Song[d], B.A. Sun[e], G. Wang*[,a], Q.J. Zhai[a], K.C. Chan[f], W.H. Wang[g]

[a]Laboratory for Microstructures, Shanghai University, Shanghai 200444, China

[b]School of Materials Science and Engineering, Anhui University of Technology, Ma'anshan 243002, China

[c]School of Materials Science and Engineering, Southeast University, Nanjing 210096, China

[d]State Key Laboratory of Metal Matrix Composites, School of Materials Science and Engineering, Shanghai Jiao Tong University, Shanghai 200240, China

[e]Department of Mechanical and Biomedical Engineering, City University of Hong Kong, Hong Kong

[f]Department of Industrial and Systems Engineering, The Hong Kong Polytechnic University, Hong Kong

[g]Institue of Physics, Chinese Academy of Sciences, Beijing 100190, China

*Corresponding author.g.wang@shu.edu.cn

Abstract

Due to the localization in space and the transience in time, investigations on the shear bands in metallic glasses are extremely difficult. The liquid-like layer frozen on fracture surfaces suggests a decreased viscosity in the shear band. Whether it is resulted from locally heating remains controversial. In this paper, the temperature rise in shear bands is profiled as a function of the duration of shear banding event, the distance from the shear band center and the thickness of shear band. The elastic energies released from the specimen and the testing machine are estimated regarding the serrations with different load drops in the compressive load–displacement curve of a Zr-based metallic glass. The duration of shear event and the released energy by serration are the two main factors determining the temperature rise in shear bands. It is found that both “cold” and “hot” shear bands are attainable. Then the sliding speed, the viscosity and the crystallization probability of shear band are studied. These results can help to better understand and describe the operation of shear band in a quantified and analytical way.

Key words: metallic glass, shear softening, shear band, temperature rise, heat diffusion

1. Introduction

Although various parameters (e.g. Poisson's ratio [1-4], free volume [5-7], structure heterogeneity [8-10], local symmetry [11]) have been extensively proposed and argued in identifying the plasticity of metallic glasses (MGs), a broad consensus is that the plastic deformation in MGs is truly and wholly dominated by shear bands [12-13]. The proliferation of shear bands is considered as the necessary prerequisite for the plasticity in MGs [8]. The shear band itself, therefore, has been investigated from different aspects [12-13]. First and foremost, the temperature in an operating shear band is supposed to rise as a result of locally heating [13], with an estimated range from 0.05 K based on nanoindentation tests [14] to 900 K as suggested from tension tests [15]. Using a fusible coating, Lewandowski *et al.* [16] estimated that the temperature rise could approach a few thousand kelvin, which was usually thought to result in melting of the material in the shear band, thus leading to prominent vein patterns and liquid droplets on the fracture surface of fractured MGs. Wright *et al.* [17-19] believed that the final fracture process, rather than the shear event, results in melting on the fracture surface [19] because the temperature rise was no more than 209 K in the shear band [17], which was not high enough to melt the alloy.

A critical factor that has to be considered when trying to estimate the temperature rise is the thickness of the shear band, which is closely connected with the volume and therefore the heat capacity of the shear band. However, up to date, the exact value of the thickness is still under debate [20]. It was found that the shear band thickness was 10~20 nm in $Fe_{40}Ni_{40}B_{20}$ MG [21], and about 100 nm in $Ni_{50}Pd_{30}P_{20}$ MG [22], based on transmission electron microscopy (TEM) observations. In comparison, the liquid-like layer on the fracture surface of failed MGs is usually several micrometers thick according to scanning electron microscopy (SEM) observations [13]. Nevertheless, the thickness of a single shear band formed in a uniaxially compressed $Zr_{69.5}Cu_{12}Ni_{11}Al_{7.5}$ MG was measured to be 160 μm by nanoindentation [23]. Clearly, the discrepancy is considerable.

Furthermore, the duration of a shear banding event is another factor affecting temporarily temperature rise, and is also still under dispute [13]. It has been reported to be 560 μs as measured by high frequency imaging at 12.5 kHz [19]. An upper bound of the duration, 2~6 ms, was also observed by high frequency imaging, which was consistent with the displacement–time relation for a steady-state shear in compression [24], [25]. Moreover, the low bound of the duration of the shear banding event was reckoned to be ~1 ns [16]. It is evident that the shear banding duration has a very large

range that covers six orders of magnitude between the upper bound and low bound values.

As a consequence, we can pose a question: how hot are the shear bands in metallic glasses? To address this issue, the constitutive equations concerning the above two critical variables, i.e., the thickness of the shear band and the duration of shear-banding event, the intrinsic properties (e.g. thermal diffusivity) of MGs, and the extrinsic conditions (e.g. testing-machine stiffness) of the measurements are required to give a reasonable evaluation of the temperature rise. This is of importance not only for understanding the dynamics of shear banding but also for toughening metallic glasses.

In this paper, the energy transferred from the testing machine and the elastically strained matrix of the MG to the thin shear band is investigated. The energy absorbed by the shear band is partly consumed to increase the temperature of shear-band material, and partly diffuses outside the shear band as heat. The temperature profile around the shear band is determined. Then the comprehensive examination on the sliding speed, the viscosity of the operating shear band as well as the probability of crystallization in the shear band is made. The compression tests of a $Zr_{41.25}Ti_{13.75}Ni_{10}Cu_{12.5}Be_{22.5}$ (at%) MG (Vitreloy 1) are used to confirm the theoretical analysis.

2. Experimental methods

Vitreloy 1 alloy ingot was fabricated by arc-melting pure metals under a Ti-gettered purified argon atmosphere, followed by suction casting into a copper mold to form a rod of 2 mm in diameter and 65 mm in length. Its glassy structure was ascertained by X-ray diffraction (XRD). Compression test specimens were cut from the as-cast MG sample by a diamond saw with cooling water, having a height of 4 mm and a diameter of 2 mm. Compression tests were conducted using an Instron 8562 machine at a strain rate of 2.5×10^{-4} s^{-1}. APHENOM^{TM} G2, FEI, a scanning electron microscope (SEM), was used to observe the fractography.

3. Results and discussion

3.1. Energy conservation in a shear banding event

At room temperature, the shear banding events in malleable MGs (e.g., Pt- [1] and Zr- [8] based MGs) are characterized as a series of serrations in the plastic regime of the compression load–displacement curves at a quasi-static strain rate [12,26]. Usually, these serrations are conceptually

ascribed to the successive formations of multiple shear bands [1,8], or intermittently sliding of a single primary shear band [27-28]. Recently, both ex-situ [27-28] and in-situ [19] observations have corroborated that the plastic deformation of MG proceeds mainly by iterative sliding of one part of the specimen over another along a primary shear band. Few secondary shear bands are able to form unless the primary shear band is arrested artificially [8,29]. Therefore, in the present study, one shear banding event is phenomenally simplified to correspond to one serration in the load–displacement curve. Theoretically, the shear band can propagate in two possible ways, i.e., in simultaneous manner or in progressive manner [13]. Recent in-situ video filmed by high frequency camera, however, demonstrates the simultaneous way is more preferable [19], at least within the revolution limit of the employed camera. So, the shear is treated in the simultaneous manner in the present study.

A representative load–displacement curve for the compression test of a malleable MG is illustrated in Fig. 1a. According to the amplitude size of the serrations, we classify the serrations into three types, i.e., medium serration (i.e., Nos. 1 and 2), large serration (i.e., No. 3), and small serration (i.e., No. 4), as marked by red arrows in Fig. 1a. The elastic energy, ΔE, released from the testing system during a shear banding event, is sketched in Fig. 1a, and can be expressed as,

$$\Delta E = \frac{1}{2k}(F_p^2 - F_v^2), \quad (1)$$

where $k = k_s k_m/(k_s+k_m)$ ($ks=EA/l$, E is Young's modulus, A is the cross-section area of the specimen, and l is the length of the specimen; k_m is the stiffness of the machine) [28,30], and F_p and F_v are the peak and valley load values of the serration, respectively. Thus, $\Delta F=F_p-F_v$ in Fig. 1a. In Fig. 1b, the testing machine can be simplified as a spring because it is actually not ideally rigid [31-32].

If the temperature of the shear band increases by ΔT above the ambient temperature (~300 K), the required energy, ΔE_H, must be:

$$\Delta E_H = 2A'h\rho c\Delta T, \quad (2)$$

where h is the half thickness of the shear band (see details in Fig. 1c), ρ is the density, c is the specific heat of the material. Because the shear band slides along the shear plane in a simultaneous way through the sample, $A' = A/\sin(\theta)$ (θ is the angle between the shear plane and the loading direction, as shown in Fig. 1b). If the shear-banding event is fast enough, the heat conduction will be negligible, which is so-called adiabatic shear [33]. However, the shearing process cannot be fully adiabatic because the heat diffusion is, more or less, inevitable [13,16,34-35,41-42] Regarding the heat diffused outside the shear band, Q, during the shear banding event, we can easy to obtain

$$\Delta E_H = \alpha \Delta E - Q, \tag{3}$$

where α is a dimensionless factor considering the fraction of ΔE transferred into the shear band [28-33].

3.2. Model of a shear band with zero thickness

Eqs. (1), (2), (3) provide a necessary but rough description of the shear-banding event based on energy balance. Lewandowski and Greer idealized the shear band with a zero thickness, and treated it as a planar heat source [16]. They then gave the temperature rise, ΔT, as a function of time, t, and distance, x, expressed as

$$\Delta T = \frac{H}{2\rho c\sqrt{\pi \kappa t}} \exp(-\frac{x^2}{4\kappa t}), \tag{4}$$

where H is the heat content per unit area, and κ is the thermal diffusivity. Clearly, at the position of x=0 and the initial time of t = 0, the temperature rise, ΔT, is a singularity, i.e., $\Delta T \to \infty$. This indicates two points. One is that the idealization, i.e., the zero thickness of shear band, is not a true physical fact, and the other one is that the energy transfer from the sample–machine system into the band is neither adiabatic nor instantaneous. Keeping the thickness of the shear band as zero, and the elapsed time of the energy transfer to be δt, one can profile the temperature rise as a function of t as [19], [35], [42]

$$\Delta T = \frac{f}{K}\left[\sqrt{\frac{\kappa t}{\pi}} \exp(-\frac{x^2}{4\kappa t}) - \frac{x}{2}\operatorname{erfc}(\frac{x}{2\sqrt{\kappa t}})\right] \qquad (t<\delta t), \tag{5}$$

where f is the heat flux per unit area per unit time, K is the thermal conductivity, and erfc is the complementary error function. Wright *et al.*[19] suggested

$$f = \tau \dot{u}, \tag{6}$$

where τ is the yield shear stress, and the sliding speed of the operating shear band, $\dot{u}$, is usually less than 10^{-3} m/s. Accordingly, it can be roughly estimated that there is no significant temperature rise in the center of the shear band, i.e., x=0. However, a number of studies show that the significant temperature rise could occur in the regions of dense shear bands [35], [42], especially near to the fracture surface [25], [36-37], [43-44].

3.3. Consideration of finite thickness of a shear band

3.3.1. Heat diffusion after energy transfer

As illustrated in Fig. 1c, the thickness of the shear band, $2h$, is never less than 10 nm according

to previous result [20]. If the elapsed time of the energy transfer, δt, is neglected, it means that the adiabatic heat transfer is already completed at the initial time of t=0. Then, we have,

$$T_0=\frac{E_T}{2hA'\rho c} \qquad (x < h) \tag{7a}$$

$$T_0=0 \qquad (x > h). \tag{7b}$$

When $t > 0$, the heat in the shear band begins to diffuse out, and the temperature rise, ΔT, is given as [38], [45],

$$\Delta T = \frac{\alpha\Delta E}{4hA'\rho c}\left[erf(\frac{h-x}{2\sqrt{\kappa t}}) + erf(\frac{h+x}{2\sqrt{\kappa t}})\right], \tag{8}$$

where erf is an error function. It can be noticed that the evolution of ΔT with position, x, and time, t, in Eq. (8) considers the finite thickness of the shear band, which is greatly different from those in Eqs. (4), (5).

To check the model above proposed for an operating shear band, compression tests on Vitreloy 1 are performed. The machine stiffness, k_m (~8.03×107 N/m), is measured from the load–displacement curve without the specimen [30]. The serrations in the compressive load–displacement curve of Vitreloy 1 are shown in Fig. 2a. The load drops, ΔFs, of the serrations are calculated to be in a range from 5.2 to 213.4 N. The corresponding values of ΔE, calculated by Eq. (1) range from 8.9×10^{-4} to 3.7×10^{-2} J. Since the α value is usually taken as 0.9 in Eq. (3) [28], [34], [41], ΔE must lie between 8.01×10^{-4} and 3.33×10^{-2} J. The heat content per unit area, H, is estimated to be 0.4~2.2 kJ·m^{-2} as given in Ref. [16]. In the present study, when a mature shear band slips through the specimen with $\theta \approx 42^{\circ}$ (see Fig. 6a), the total heat is $HA' = 0.2 \sim 1.1\times10^{-2}$ J that is within the estimated range (from 8.9×10^{-4} to 3.7×10^{-2} J). In addition, it is worth noting that the load drops of the serrations in Region I, which is marked in Fig. 2a, are about 80 N, as shown in Fig. 2b. After a displacement of 0.23 mm, i.e., in Region II of Fig. 2a, the load drops are not less than 150 N, as shown in Fig. 2c. Therefore, the elastic energy released in each serration of Region I is about half of that in Region II. Fig. 2d shows the released elastic energy values for all the serrations.

For Vitreloy 1, ρ = 6125 kg·m^{-3}, c = 420 J·kg^{-1}, κ = 3.5×10^{-6} m^2·s^{-1}, and $K = \rho c\kappa$ [39], [46]. Since these parameters only change slightly with temperature [40], [47], we treat these parameters as constants. According to Eq. (7a), when the ΔE value is chosen as the maximum value of 3.33×10^{-2} J, and the h value is the smallest value of 5 nm, ΔT is as high as 2.5×105 K at t=0 s, which is not

reasonable. To make sense in reality, the h value should be at least 500 nm so that the initial ΔT has a value of 2.5×103 K. If the liquidus temperature of Vitreloy 1 (996 K) [40], [47] is the upper bound of the temperature, the h value will be 1.8 μm, and means that the thickness of the shear band is 3.6 μm, slightly thicker than the liquid-like layer on the fracture surface of MGs [13]. Based on Eq. (8), the temperature rise, ΔT, as a function of time, t, and distance, x, is mapped with h=500 nm and ΔE= 3.33×10^{-2} J in Fig. 3a. Fig. 3b shows the temperature profiles with the x value at different times. At t=1 ns, the temperature rise, ΔT, decreases with increasing x value, especially, at x=250 nm, where the ΔT value commences to decrease dramatically. At t=10 ns, the ΔT value exhibits a similar trend as compared to that at t=1 ns. When t=100 ns, the ΔT value becomes more uniform with x. At t=200 ns, the temperature rise profile has almost no change with the x value, which means that the heat diffusion practically finishes in ~200 ns. This temperature rise profile is consistent with the early studies [16], [35], [41-42], [48]. Consequently, it can be reasonably inferred that if the shear-banding event lasts longer than 200 ns, adiabatic shear will never be available.

3.3.2. Concurrence of energy transfer and heat diffusion

Logically, the stored energy in the system cannot be released and transferred unless the shear band slides and causes a stress relaxation throughout the specimen along the loading direction. The shear-band material can release the elastic energy, and therefore heat itself with this energy when its stress level, marked by the load drop in the load–displacement curve, is falling. After that, the temperature of the heated shear band begins to decrease because the heat can diffuse into the surrounding matrix. As a result, the energy transferred from testing system to the shear band concurs simultaneously with the heat diffusion from the heated shear band into the cool surrounding matrix. When the energy transfer is completed, the shear band cannot stop sliding instantaneously due to the inertia. Therefore, the shear-banding event will outlive the energy transfer process. However, the continued sliding due to the inertia cannot last for a long time because of the shear resistance in the band and the weakened driving force caused by the decreased stress level [13]. Accordingly, our estimation of the elapsed time, which treats the timespan of energy transfer as the duration of the shear-banding event, is acceptable. The energy release and transfer in a compressed specimen along the compressive loading axis must proceed at the speed of a longitudinal sound wave [42], [49]. Therefore, the elapsed time of the energy transfer, δt, can be evaluated by,

$$\delta t \sim \frac{l'}{v_l}, \tag{9}$$

where l' is the distance from the end of sample to the center of shear band, so , and v_l = 5174 ms^{-1} is the speed of the longitudinal sound wave in Vitreloy 1 [50]. The relation of Eq. (9) is well documented in Appendix. The δt value can be estimated to be 200–400 ns, which rules out the possibility of adiabatic shear.

When the elastic energy stored in the system is being released and transferred into the shear band, the heat is being diffused out of the shear band due to the temperature difference. The shear band is so thin that it can be considered to be uniform along the thickness direction. As such, the energy released in the shear band per unit volume and per unit time on average, ω, is,

$$\omega = \frac{\alpha E_T}{2hA'\delta t}. \tag{10}$$

So we have a one-dimensional differential equation for the conduction of heat,

$$rc\frac{\partial \mathrm{D}T}{\partial t} = K\frac{\partial^2 \mathrm{D}T}{\partial x^2} + w \qquad (x < h,\ 0 < t < dt) \tag{11a}$$

$$rc\frac{\partial \mathrm{D}T}{\partial t} = K\frac{\partial^2 \mathrm{D}T}{\partial x^2} \qquad (x > h,\ 0 < t < dt). \tag{11b}$$

The analytical solutions to Eqs. (11a) and (11b) have expressions as following [38], [45],

$$\Delta T = \frac{\kappa\omega t}{K}\left[1 - 2i^2\, erfc(\frac{h-x}{2\sqrt{\kappa t}}) - 2i^2\, erfc(\frac{h+x}{2\sqrt{\kappa t}})\right] \quad (0 < x < h, 0 < t < \delta t). \tag{12a}$$

$$\Delta T = \frac{2\kappa\omega t}{K}\left[i^2\, erfc(\frac{x-h}{2\sqrt{\kappa t}}) - i^2\, erfc(\frac{x+h}{2\sqrt{\kappa t}})\right] \quad (x > h, 0 < t < \delta t). \tag{12b}$$

Based on Eq. (14), Fig. 4 graphically presents the mapping of the temperature rise for ΔE = 3.33×10^{-2} J in the x range of 1~1000 nm. For the case of h = 5 nm and δt = 200 ns in Fig. 4a, the temperature gradually increases, and reaches the maximum value of 1662 K at t = 200 ns. Given the ambient temperature of ~300 K, the maximum temperature at the center of the shear band is 1962 K, which is much higher than the liquidus temperature (996 K) of Vitreloy 1, but significantly lower than the value of 3400~8600 K proposed in Ref. [16]. A similar temperature rise evolution also occurs in Fig. 4b, if δt = 400 ns, and the maximum temperature rise decreases to 1178 K at x = 0 at the end of shear. If the elapsed time of the energy transfer is increased by one order of magnitude, i.e., δt = 2000 ns, the temperature rise profile, as displayed in Fig. 4c, changes significantly, and the maximum value never exceeds 550 K. On the other hand, when h = 50 nm, one order of magnitude larger than that (h = 5 nm) in Fig. 4a, there is no significant difference in the temperature rise profile. For comparison, Fig. 4e shows the temperature profiles at different x values and different δt values. The

inset of Fig. 4e shows a tiny difference in the temperature rise profile between the cases of h = 5 nm and h = 50 nm. From a practical point of view, if the melted layer (marked by the dashed horizontal line) is treated as the shear band, the shear band with δt = 400 ns (green dashed vertical line) is ~10% thinner than that with δt = 200 ns (red dashed vertical line). This demonstrates that the duration of the shear-banding event, i.e., the elapsed time of energy transfer, affects the temperature rise more than the thickness of the shear band. On the other hand, the thickness of the melted layer is about 1.5 μm as marked by the vertical dashed line, which is very close to that of the liquid-like layer on the shear lip or the fracture surface [13]. Obviously, the thickness of the shear band is estimated to be much larger here than the previously presumed thickness, i.e., 10 and 100 nm. This indicates that the shear band has thickened during shear banding [13].

Once a liquid-like layer is formed in the shear band, the temperature rise, ΔT, must be higher than 696 K (= the liquidus temperature (996 K) – room temperature (300 K)). The minimum energy, ΔE, for the generation of the liquid-like layer in the shear bands (ΔT = 696 K) is calculated to be 1.37×10^{-2} J, which is marked as the dash line in Fig. 2d, when h = 5 nm and δt = 200 ns. The ΔT profile is plotted in Fig. 5, based on Eq. (14). It can be seen that most of the energies released by the serrations in Region I are less than 1.37×10^{-2} J, while the energies in Region II are almost higher than 1.37×10^{-2} J. In this case, the melted shear band, i.e., $\Delta E > 1.37\times10^{-2}$ J, can be called “hot”, and in the case of $\Delta E < 1.37\times10^{-2}$ J is “cold”. Therefore, the shear bands developing in the early stage, i.e., those enclosed in the lower-left corner in Fig. 2d, are all cold, which can be confirmed by the shear lips with smooth surfaces observed in the fractured MG [13]. Otherwise, the upper-right enclosed region in Fig. 2d marks the hot shear bands. Of course, although what fraction of the energy released by the final fracture is transferred into the shear band is unknown, ΔE should be larger than 3.33×10^{-2} J, for the load drops to zero. The temperature rise in shear-banding-crack must therefore be higher, and it causes the melting of fracture surface material or coating materials with low liquidus temperatures on the side surface, which were observed in many earlier studies [13], [15-19], [25], [32], [36-37].

3.4. Investigation on the failed specimens by SEM

The SEM observations on the fractured MG specimen are presented in Fig. 6. Fig. 6a shows an overview of the lateral surface. The specimen is sheared off at a shear angle of 42°, and few secondary

shear bands can be found near the fracture surface. This indicates that the plastic deformation proceeds mainly through the primary shear band sliding [27], [51]. Further enlarging the shear lip (marked by an arrow in Fig. 6a), one can see two distinct regions, as shown in Fig. 6b. The regions, as enclosed by yellow circles, adjacent to the lateral surface of specimen, are smooth. A high magnification image shows numerous striations with a spacing, Δu, of ~3 μm in this smooth region, as shown in Fig. 6c, which is consistent with previous results [27-28]. The smooth region presented in the shear lip implies that no significant temperature rise occurs during shear banding. However, after shear sliding approximately u_s = 300 μm away from the shear lip, marked by the red circles in Fig. 6b, vein patterns appear. The boundary between the smooth region and the vein pattern region is clearly distinguishable, as shown in Fig. 6d. These vein patterns suggest that the temperature rises at least up to the melting temperature of the MG. As indicated in the load–displacement curve in Fig. 2a, most of the serrations with larger ΔE values appear after the displacement, Δx, of 230 μm, which gives a corresponding shear displacement, $u = \Delta x/\cos 42° = 309$ μm, along the shear plane, very close to us. It is reasonable to conclude that the large energy released in the serrations is responsible for the significant temperature rise.

According to the above analysis, after yielding, when the serrations with large load drops (therefore large ΔE) appear, a smooth region cannot appear on the fracture surface but a vein pattern can. Fig. 7a represents the load–displacement curve for another Vitreloy 1 specimen. Clearly, most of the serrations in the plastic regime exhibit a load drop of more than 100 N within the plastic regime of a displacement $\Delta x \approx 85$ μm, and therefore the calculated $\Delta E > 2.0\times10^{-2}$ J. Fig. 7b presents a side view of the deformed Vitreloy1 MG, and a shear lip is marked by a circle. After the SEM observation, the deformed MG was reloaded and broken into two pieces. Further enlarging the morphology of the shear lip, a vein pattern, with no smooth region, can be observed, as shown in Fig. 7 c [35]. In addition, we find a number of molten droplets, as typically marked by small arrows in Fig. 7d, at a distance $u_d \approx 60$ μm away from the tip of the shear lip as circled in Fig.7c. These droplets are always indicator of high temperature [13]. More important, some tiny "tails", as marked by large arrows in Fig. 7d, are found to draw from the surface. These tails are obviously the frozen melts of the shear-band material. Note that u_d is only about half of $\Delta x/\cos\theta \approx 120$ μm (θ taken to be 45°). So the tails, which are absolutely not caused by the final fracture, are unquestionable evidence of significant

temperature rise in shear band prior to the final fracture of the MG. On the other hand, if the released energies of all serrations are small, only cold shear bands are developed, which means that the shear lip will be smooth and/or striated rather than veined, and this has been experimentally confirmed by Song *et al*. [27].

3.5. Intrinsic properties of a shear band

For crystalline metals, thermal softening outweighs strain hardening at very high strain rates, typically ~10^3 s^{-1}, which results in a shear localization in an adiabatic manner [33]. The temperature rise, therefore, is appreciable in the shear band. However, there is no work hardening mechanism in monolithic MGs. Thus, the plastic strain cannot spread out globally, and the strain localization, i.e., shear banding, is inevitable at temperatures well below the glass transition temperature, and is almost independent of the strain rate. As a result, both cold and hot shear bands are available in MGs. For cold shear bands, some striations on the shear lip are observed in Fig. 6c. The averaged striation spacing is measured to be 3 μm. Striation is the trace leaved by one shear slip driven by the stress drop in a serration event [27]. Since the formation of the striation is an elastic energy dissipation process, its elapsed time is roughly equivalent to the elastic recovery time of the specimen during the stress drop, which is estimated to be 200 ns (see Appendix). Thus, the average sliding speed, v_{sb}, can be estimated by $v_{sb} = \Delta u/\delta t \approx 3$ μm/200 ns = 15 m/s. Hot shear bands usually do not show distinguishable traces, such as striations. The displacement is about $2\Delta u$ because of the load drops in hot shear bands is almost twice larger than that in cold shear bands, as shown in Fig. 2b and c. Hence, the sliding speed should be around 30 m/s, that is one to four orders of magnitude higher than the values reported in early studies [18], [24], [45], [52]. Considering the hot operating shear band at v_{sb} = 30 m/s, one can obtain the ΔT_{max} value of 1564 K at the center of the shear band according to Eq. (5), which approaches 1662 K based on Eq. (12). This confirms that the sliding speed of the operating shear band, estimated by our model, is essentially accurate.

The viscosity, η, of the operating shear band is calculated by [12],[24],

$$\eta = \frac{\tau}{\dot{\gamma}} , \tag{13}$$

where $\dot{\gamma} = \dot{u}_{sb} / 2h$ is the shear strain rate. Since v_{sb} = 15 ~ 30 m/s, and h = 5 ~ 50 nm, the viscosity, η, can be estimated to be 0.3 ~ 6.5 Pa·s that is much lower than the reported value of 10^4 ~ 10^5 Pa·s in a Zr-based MG [24]. However, since the temperature in the hot shear band substantially exceeds

the melting point of MGs, the viscosity of the shear band should be of the order of 10^{-3} Pa·s [46], [53]. Obviously, there is a discrepancy. In fact, the viscosity of metal melts follows the Arrhenius law [47], [54],

$$\eta = \eta_0 \, exp(\frac{\Delta G}{RT}), \tag{14}$$

where η_0, ΔG, R, and T are the pre-exponential factor, the activation energy, the gas constant, and the temperature, respectively. For most liquid metals, the ΔG value usually lies in the range of 10^3~10^4 J/mol at their melting temperatures [47], [54]. Moreover, the activation energy is usually proportional to the pressure, so the Arrhenius relation can be modified to be,

$$\eta = \eta_0 \, exp(\frac{G+PV}{RT}), \tag{15}$$

where $P = (\sigma_{xx} + \sigma_{yy} + \sigma_{zz})/3$ is the hydrostatic pressure, and $V = 9.79\times10^{-6}$ m^3/mol (Vitreloy 1) is the molar volume [48], [55]. When yielding occurs, $\sigma_{xx} = \sigma_y \sin\theta\cos\theta$ (σy ~ 2.0 GPa is yield stress of Vitreloy 1) and $\sigma_{yy} = \sigma_{zz} = 0$ in compression. So, the PV value is estimated to be 3.2×10^3 J/mol that is comparable to the value of E. As a result, the pressure can increase the viscosity of the melt. This pressure effect has been noticed in the fracture behavior of MGs under compression and tension tests [49], [56], which is the possible reason resulting in the compressive fracture strength being slightly higher than the tensile strength. Although the shear dilatation can also reduce the viscosity in MGs, it mainly functions when the temperature rise in shear band is not so significant, especially during the structure disordering or rejuvenation process induced by the stress concentration prior to the maturity of a shear band [13]. Therefore, heating has a much more substantial effect on the reduction of the viscosity than the effect from the dilatation, which can be seen in Fig. 7c and d.

It must be pointed out that neither exothermal heat for crystallization nor endothermal heat for melting is taken into consideration in our model. As evaluated in Eq. (12), the heating rate is no less than 10^8 K/s for the formation of a hot shear band. If the heating rate is larger than 200 K/s, crystallization can be entirely avoided, and therefore no latent heat is absorbed for melting during the continuously heating process in Vitreloy 1 [57-58]. Apart from the heating process, the ensuing cooling process also can cause crystallization if the cooling rate is not high enough. Since the energy transfer is finished when $t = \delta t$, $\omega = 0$ if $t > \delta t$ in Eq. (11), the following cooling process can be described by solving Eq. (11) with the initial condition presented by the black curve in Fig. 4e, i.e., h = 5 nm and δt = 200 ns. Fig. 8a profiles the whole evolution of the temperature rise around the shear

band within 1600 ns. Fig. 8b plots the temperature rise, ΔT, as a function of time, t, at the center of shear band, which shows that the temperature rise reaches the peak value of 1662 K at 200 ns. After the peak value, the ΔT value dramatically decreases to 600 K in the next 200 ns, and then further decreases to 310 K in the following 1200 ns. The ΔT value of 310 K means that the temperature at the center of shear band is approximately 610 K, which is already lower than the glassy transition temperature (~620 K) of Vitreloy 1. During this cooling process, the average cooling rate is no less than 108 K/s. Regarding that the critical cooling rate required to form the glassy phase in Vitreloy 1 is ~2 K/s [57], one can see that it is impossible to induce crystallization in MGs. However, crystallization induced by deformation has widely been observed in bending of $Cu_{50}Zr_{50}$ ribbons [59], compression of $Ni_{50}Pd_{30}P_{20}$ [22], cold-rolling of Al–Y–Fe [60], and nanoindentation of $Zr_{52.5}Cu_{17.9}Ni_{14.6}Al_{10}Ti_5$ [14]. From the view of our model, only the thermal effect is insufficient to cause crystallization because of super-high heating and cooling rates. If the atomic-scale crystalline nuclei already pre-existed in the as-prepared MGs prior to deformation [62], these nuclei could easily grow and coarsen in virtue of accumulated heating caused by many shear-banding events [61]. On the other hand, this very fast cooling rate cause the melted shear-band material to be solidified within the response time of the testing machine [13], and in turn stops shear banding again in compression test. Therefore, even though the temperature in shear band is much higher than the liquidus temperature of the MG, the sample doesn't simply fail.

4. Conclusions

In the present study, the deformation-induced temperature rise is profiled based on a simple method, which can estimate the energies released from specimen and testing machine in the shear-banding events of plastic deformed MGs. According to the transfer and balance of the energy, local heating and the temperature rise in a shear band are quantitatively studied with consideration of the thickness of the shear band, and the elapsed time of the energy transfer. Cold and hot shear bands are found to be both available during the plastic deformation in MGs, depending on the amount of the released energy in each serration and the duration of the shear banding event. The hydrostatic pressure caused by the normal stress on the shear plane increases the viscosity of the operating hot shear band to be on the order of 1 Pa s.

Acknowledgements

The authors thank Prof. Eckert and the reviewers for their critical comments which in turn help to improve our manuscript greatly. This work is supported by grants from MOST (No. 2015CB856800), NSFC of China (Nos. 51201001, 51171098, and 51222102), the RGC of the Hong Kong SAR (No. PolyU511211), the China Postdoctoral Science Foundation (No. 2014M561550), and the Programs for Professor of Special Appointment (Eastern Scholars) at Shanghai Institutions of Higher Learning.

References

[1] Schroers J, Johnson WL. Phys Rev Lett 2004;93:255506.

[2] Lewandowski JJ, Wang WH, Greer AL. Philos Mag Lett 2005;85:77.

[3] Gu XJ, McDermott AG, Poon SJ, Shiflet GJ. Appl Phys Lett 2006;88:211905.

[4] Poon SJ, Zhu AW, Shiflet GJ. Appl Phys Lett 2008;92:261902.

[5] Spaepen F. Acta Metall 1977;25:407.

[6] Huang YJ, Shen J, Sun JF. Appl Phys Lett 2007;90:081919.

[7] Chen LY, Fu ZD, Zhang GQ, Hao XP, Jiang QK, Wang XD, Cao QP, Franz H, Liu YG, Xie HS, Zhang SL, Wang BY, Zeng YW, Jiang JZ. Phys Rev Lett 2008;100:075501.

[8] Liu YH, Wang G, Wang RJ, Zhao DQ, Pan MX, Wang WH. Science 2007;315:1385.

[9] Jiang MQ, Dai LH. Philos Mag Lett 2010;90:269.

[10] Yu HB, Shen X, Wang Z, Gu L, Wang WH, Bai HY. Phys Rev Lett 2012;108:015504.

[11] Peng HL, Li MZ, Wang WH. Phys Rev Lett 2011;106:135503.

[12] Schuh CA, Hufnagel TC, Ramamurty U. Acta Mater 2007;55:4067.

[13] Greer AL, Cheng YQ, Ma E. Mater Sci Eng R 2013;74:71.

[14] Kim JJ, Choi Y, Suresh S, Argon AS. Science 2002;295:654.

[15] Liu CT, Heatherly L, Easton DS, Carmichael CA, Schneibel JH, Chen CH, Wright JL, Yoo MH, Horton JA, Inoue A. Metall Mater Trans A 1998;29A:1811.

[16] Lewandowski JJ, Greer AL. Nat Mater 2006;5:15.

[17] Wright WJ, Schwarz RB, Nix WD. Mater Sci Eng A 2001;319-321:229.

[18] Wright WJ, Samale MW, Hufnagel TC, LeBlanc MM, Florando JN. Acta Mater 2009;57:4639.

[19] Wright WJ, Byer RR, Gu XJ. Appl Phys Lett 2013;102:241920.

[20] Zhang Y, Greer AL. Appl Phys Lett 2006;89:071907.

[21] Donovan PE, Stobbs WM. Acta Metall 1981;29:1419.

[22] Wang K, Fujita T, Zeng YQ, Nishiyama N, Inoue A, Chen MW. Acta Mater 2008;56:2834.

[23] Pan J, Chen Q, Liu L, Li Y. Acta Mater 2011;59:5146.

[24] Song SX, Nieh TG. Intermetallics 2009;17:762.

[25] Slaughter SK, Kertis F, Deda E, Gu X, Wright WJ, Hufnagel TC. Appl. Mater 2014;2:096110.

[26] Sun BA, Pauly S, Hu J, Wang WH, Kühn U, Eckert J. Phys Rev Lett 2013;110:225501.

[27] Song SX, Bei HB, Wadsworth J, Nieh TG. Intermetallics 2008;16:813.

[28] Sun BA, Pauly S, Tan J, Stoica M, Wang WH, Kühn U, Eckert J. Acta Mater 2012;60:4160.

[29] Wang ZT, Pan J, Li Y, Schuh CA. Phys Rev Lett 2013;111:135504.

[30] Han Z, Wu WF, Li Y, Wei YJ, Gao HJ. Acta Mater 2009;57:1367.

[31] Yang Y, Ye JC, Lu J, Liaw PK, Liu CT. Appl Phys Lett 2006;88:221911.

[32] Cheng YQ, Han Z, Li Y, Ma E. Phys. Rev. B 2009;80:134115.

[33] Bai Y, Dodd B. *Adiabatic Shear Localization: Occurrence, Theories, and Applications* (Pergamon, Oxford, 1992).

[34] Park KW, Lee CM, Wakeda M, Shibutani Y, Falk ML, Lee JC. Acta Mater 2008; 56:5440.

[35] Levaché B, Bartolo D, Phys. Rev. Lett 2014; 113:045501.

[36] Mukherjee S, Schroers J, Johnson WL, Rhim WK, Phys. Rev. Lett 2005;95:245501.

[37] Liu YH, Wang D, Nakajima K, Zhang W, Hirata A, Nishi T, Phys. Rev. Lett 2011;106:125504.

[38] Ye JC, Lu J, Liu CT, Wang Q, Yang Y, Nat. Mater 2010;9:619.

[39] Ding J, Patinet S, Falk ML, Cheng YQ, Ma E, Proc. Nat. Acad. Sci. USA 2014;111:14052.

[40] Wang G, Mattern N, Bednarčík J, Li R, Zhang B, Eckert J, Acta Mater 2012;60:3074.

[41] Yang B, Liu CT, Nieh TG. Appl Phys Lett 2006;88:221911.

[42] Georgarakis K, Aljerf M, Li Y, LeMoulec A, Charlot F, Yavari AR, Chornokhvostenko K, Tabachnikova E, Evangelakis GA, Miracle DB, Greer AL, Zhang T. Appl Phys Lett 2008;93:031907.

[43] Zhao JX, Zhang ZF. Mater Sci Eng A 2011;528:2967.

[44] Ketov SV, Louzguine-Luzgin DV, Sci. Rep 2013;3:2798.

[45] Carslaw HS, Jaeger JC. *Conduction of heat in solids* (Oxford University Press, London, 1959), 2nd, Chapter 2.

[46] Yamasaki M, Kagao S, Kawamura Y, Yoshimura K. Appl Phys Lett 2004;84:4653.

[47] Lu ZP, Liu CT. Acta Mater 2002;50:3501.

[48] Zhao M, Li M, Zheng YF. Philos Mag Lett 2011;91:705.

[49] Meyers MA. *Dynamic behavior of materials*, (John Wiley & Sons, Inc., 1994).

[50] Wang WH. Prog Mater Sci 2012;57:487.

[51] Wang JG, Chan KC, Fan JC, Xia L, Wang G, Wang WH. J Non-Cryt Solids 2014;387:1.

[52] Klaumünzer D, Maaß R, Torre FHD, Löffler JF. Appl Phys Lett 2010;96:061901.

[53] Busch R, Masuhr A, Johnson WL. Mater Sci Eng A 2001;304-306:97.

[54] Iida T, Guthrie RIL. *The physical properties of liquid metals*, (Oxford University Press Inc. New York, 1993).

[55] Wang JQ, Wang WH, Liu YH, Bai HY. Phys Rev B 2011;83:012201.

[56] Zhang ZF, Eckert J, Schultz L. Acta Mater 2003;51:1167.

[57] Schroers J, Masuhr A, Johnson WL, Busch R. Phys Rev B 1999;60:11855.

[58] Johnson WL, Kaltenboeck G, Demetriou MD, Schramm JP, Liu X, Samwer K, Kim CP, Hofmann DC. Science 2011;332:828.

[59] Chen MW, Inoue A, Zhang W, Sakurai T. Phys Rev Lett 2006;96:245502.

[60] Hebert RJ, Perepezko JH. Metall Mater Trans A 2008;39A:1804.

[61] Shibata A, Sone M, Higo Y. Scr Mater 2010;62:309.

[62] Das J, Tang MB, Kim KB, Theissmann R, Baier F, Wang WH, Eckert J. Phys Rev Lett 2005;94:205501.

Figure Captions

Fig. 1 Sketch of shear banding event in metallic glasses. (a) Illustration of serrations with different load drops and released energies in the compressive load-displacement curve. (b) Sketch of the specimen-machine system. (c) The geometric profile of the shear band is highlighted by the orange color. 2*h* is the thickness of shear band. *x* is the distance from the shear band center. The *x* axis is perpendicular to the shear plane.

Fig. 2 The mechanical behavior of Vitreloy 1 in compression test. (a) Enlarged compressive load–displacement curve in the plastic regime. The small serrations are in the displacement range of 0.23 μm. Region I covers the serrations with small load drops (ΔF < 80 N). Region II covers the large drops (ΔF > 100 N). (b) Further enlarged serrations in Region I of (a). (c) Further enlarged serrations in Region II of (a). (d) The elastic energies released by specimen–machine system in all serrations as a function of the displacement.

Fig. 3 The temperature rise as a function of time and distance according to Eq. (8) with ΔE = 3.33×10^{-2} J and h = 5 nm in Vitreloy 1. (a) The temperature rise is mapped in the range of 1~1000 nm and 1~300 ns. (b) The profiles of temperature rise along x axis at different times.

Fig. 4 The temperature rise as a function of time and distance according to Eq. (12) with ΔE = 3.33×10^{-2} J and different parameters in Vitreloy 1. (a) h = 5 nm and δt = 200 ns. (b) h = 5 nm and δt = 400 ns. (c) h = 5 nm and δt = 2000 ns. (d) h = 50 nm and δt = 200 ns. (e) The profiles of temperature rise along x axis at $t = \delta t$.

Fig. 5 The temperature rise as a function of time and distance according to Eq. (12) with ΔE = 1.37×10^{-2} J, h = 5 nm, and δt = 200 ns.

Fig. 6 SEM observations of the fracture surface of the first Vitreloy 1. (a) A side view of the fractured specimen with a fracture angle of 42°. (b) The morphology of the region marked by an arrow in (a), which shows the shear lip on the fracture surface. (c) Smooth region adjacent to the tip of the shear

lip with striation interspace of ~ 3 μm, corresponds to the region enclosed by yellow circles in (b). (d) Vein pattern on the fracture surface, which is away from the tip of the shear lip ~ 300 μm, corresponds to the region covered by red circles in (b).

Fig. 7 Observations on the second Vitreloy 1. (a) Serrations with the load drops larger than 100 N in the load–displacement curve for the first loading circle. (b) After the first loading–unloading, the shear lip, enclosed by the circle, is formed in the specimen. (c) After the second loading–unloading in which the specimen is reloaded to fracture, and SEM image shows vein patterns on the tip of shear lip, and more detailed features (molten droplets marked by small arrows and tails marked by large arrows) in the circled region is shown in (d).

Fig.8 The temperature evolution around the shear band within 1600 ns with h = 5 nm and δt = 200 ns. (a) The temperature rise map in the space range of 1000 nm. (b) The temperature rise profile at the center of shear band. ΔT reaches the peak at $t = \delta t$, then decreases rapidly.

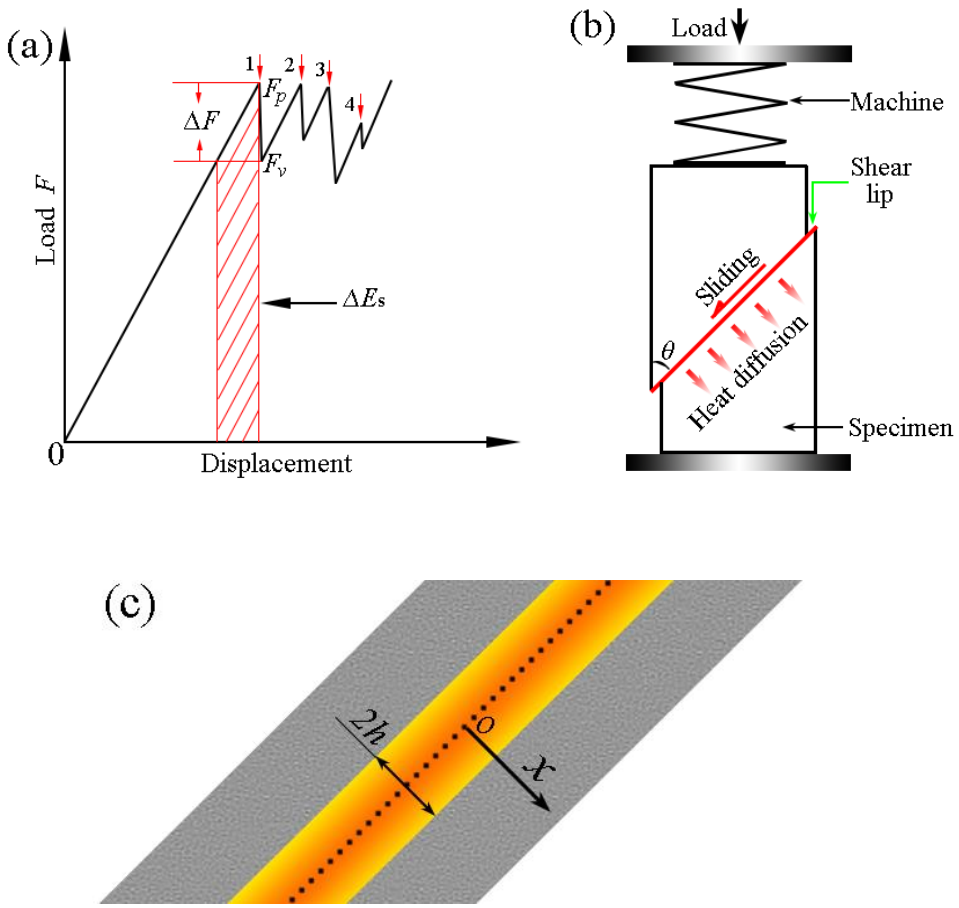

Figure 1 J. G. Wang *et al*.

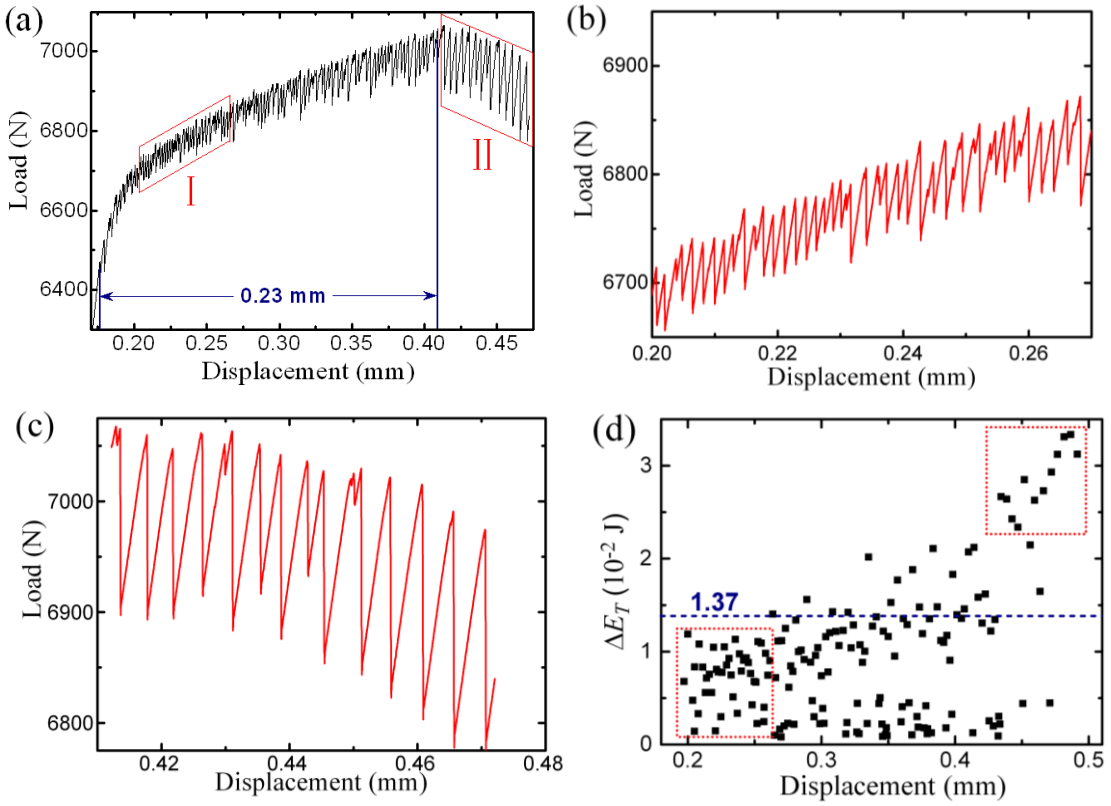

Figure 2 J. G. Wang *et al*.

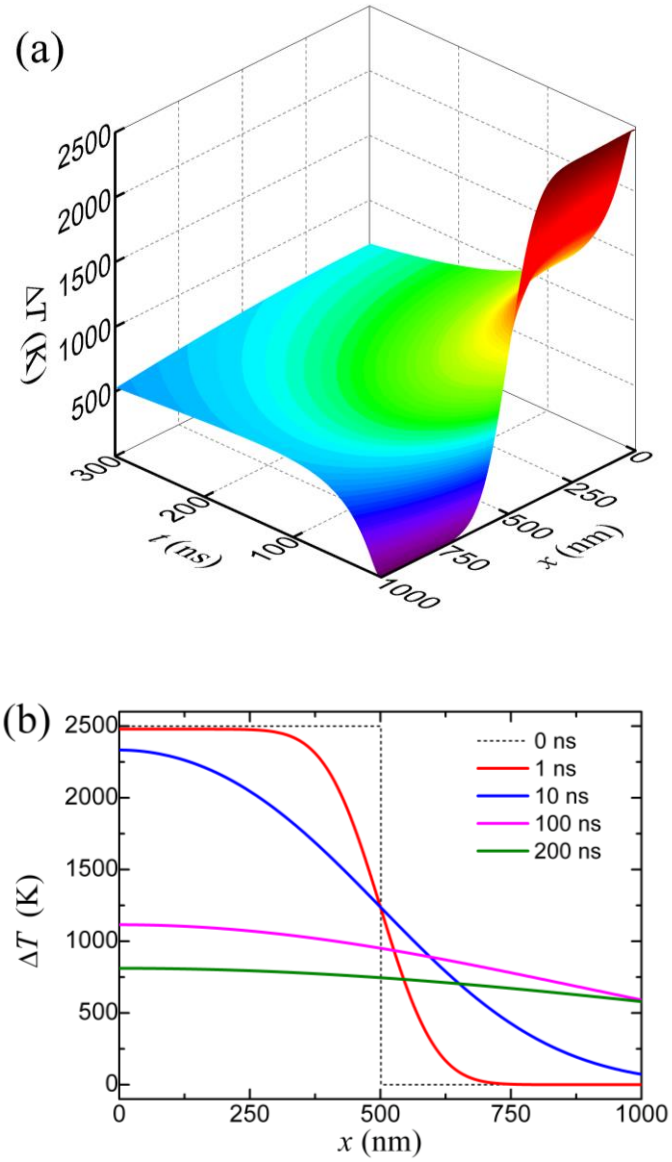

Figure 3 J. G. Wang *et al*.

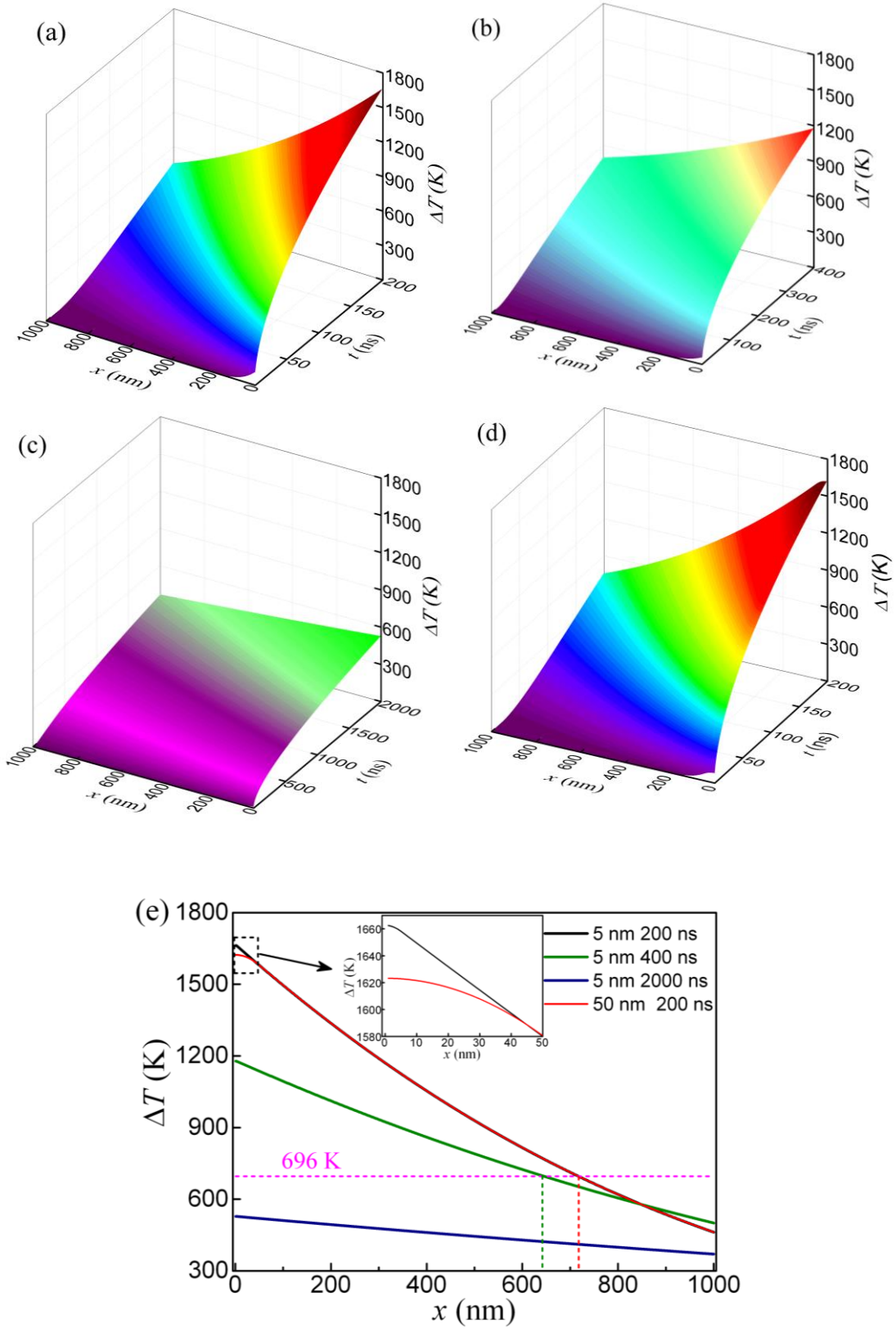

Figure 4 J. G. Wang *et al*.

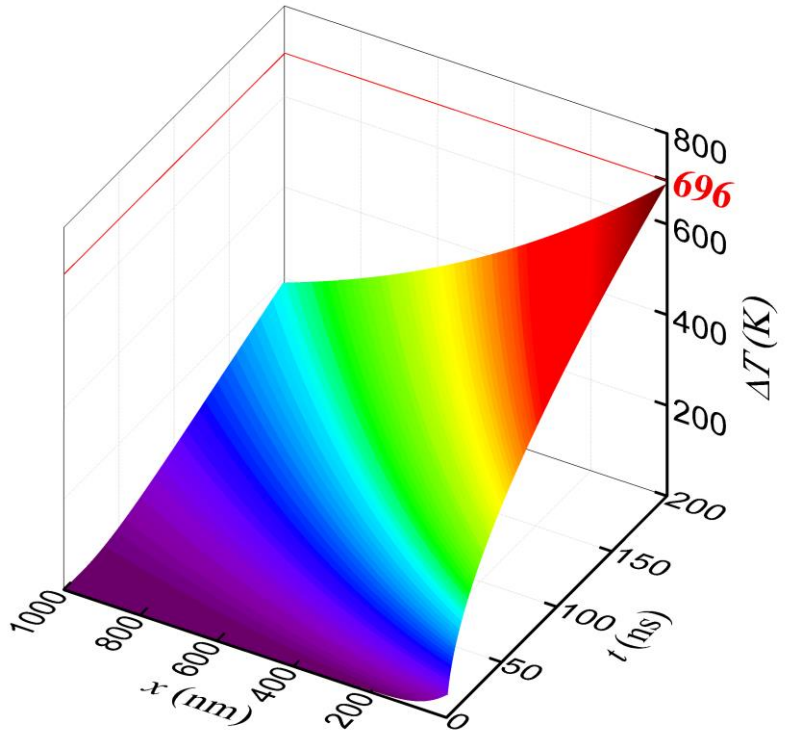

Figure 5 J. G. Wang *et al*.

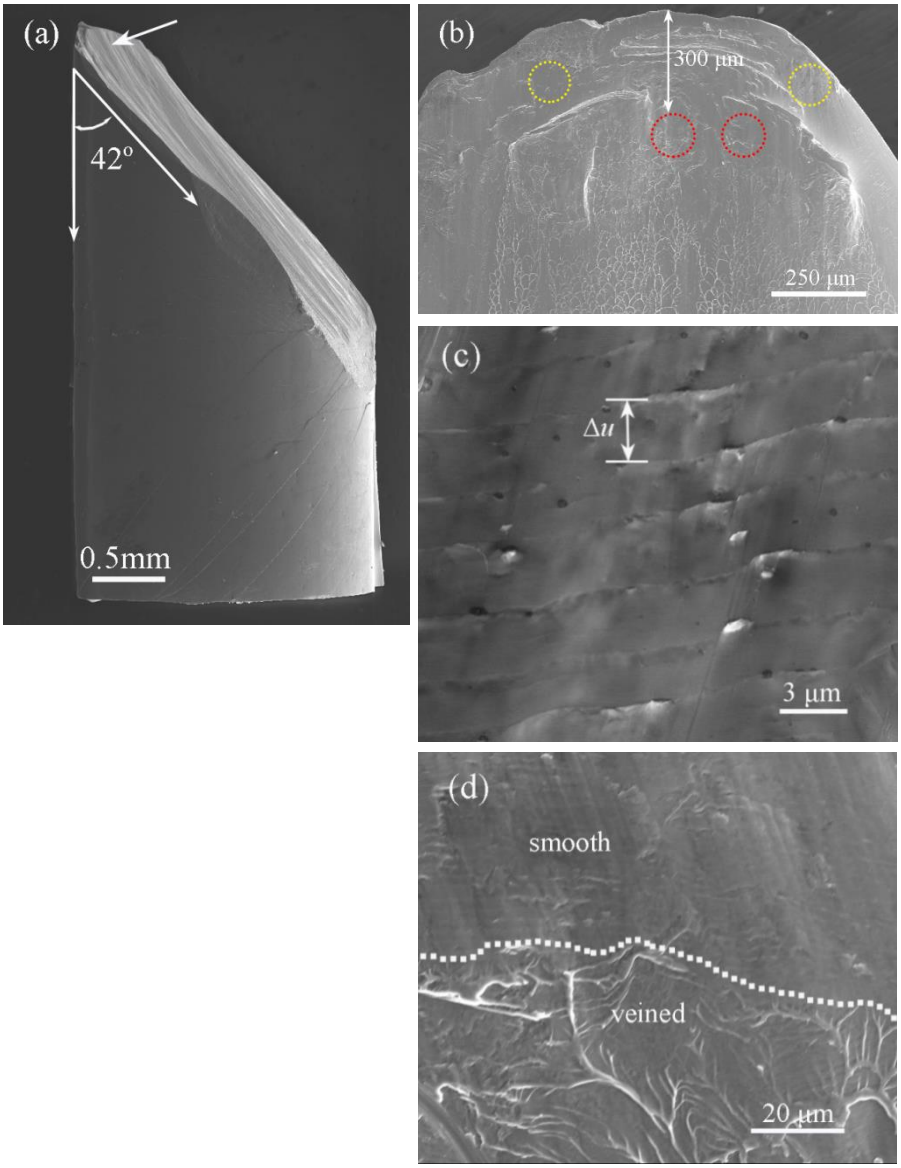

Figure 6 J. G. Wang *et al*.

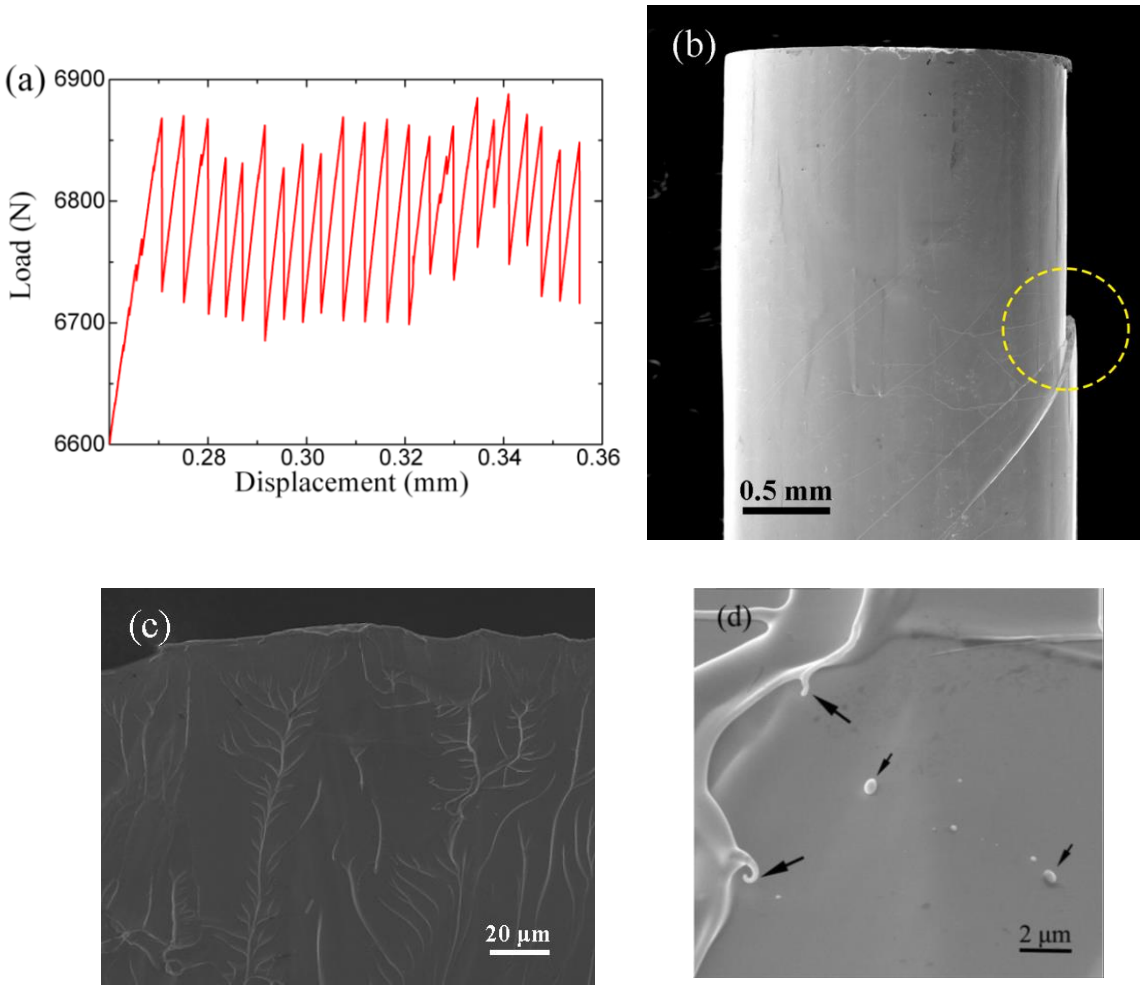

Figure 7 J. G. Wang *et al*.

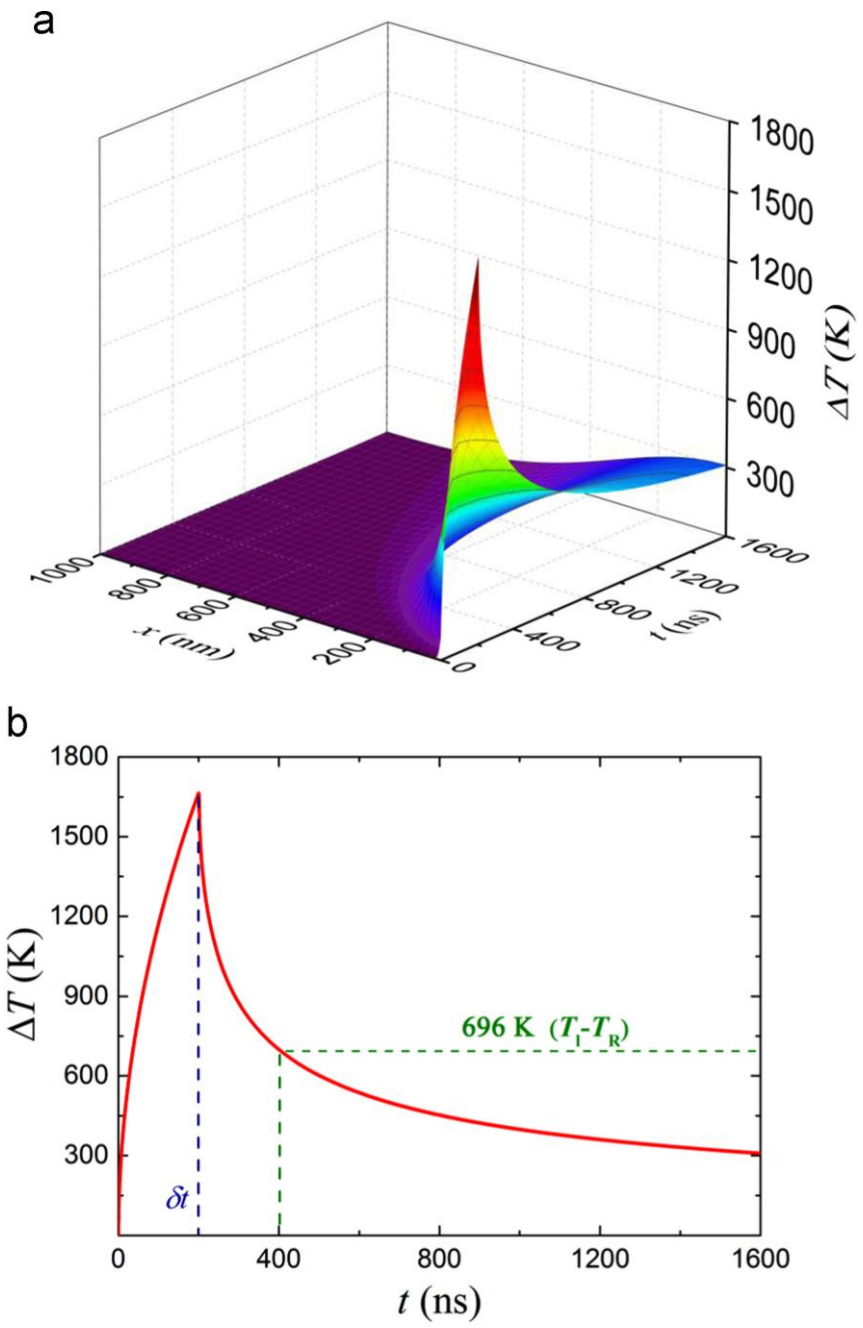

Figure 8 J. G. Wang *et al*.